Inorganic Chemistry

Communication

pubs.acs.org/IC

Solution Synthesis of Metal Silicide Nanoparticles

Joshua M. McEnaney and Raymond E. Schaak*

Department of Chemistry and Materials Research Institute, The Pennsylvania State University, University Park, Pennsylvania 16802, United States

Supporting Information

ABSTRACT: Transition-metal silicides are part of an important family of intermetallic compounds, but the high-temperature reactions that are generally required to synthesize them preclude the formation of colloidal nanoparticles. Here, we show that palladium, copper, and nickel nanoparticles react with monophenylsilane in trioctylamine and squalane at 375 °C to form colloidal Pd_2Si, Cu_3Si, and Ni_2Si nanoparticles, respectively. These metal silicide nanoparticles were screened as electrocatalysts for the hydrogen evolution reaction, and Pd_2Si and Ni_2Si were identified as active catalysts that require overpotentials of −192 and −243 mV, respectively, to produce cathodic current densities of −10 mA cm^{-2}.

Intermetallic compounds of the transition metals and silicon constitute an important and diverse family of inorganic solids that are of interest for their fundamentally interesting structures and properties, as well as for their technological applications.[1−3] Depending on their constituent metals, stoichiometries, and crystal structures, metal silicides can exhibit a range of electronic, magnetic, optical, catalytic, and mechanical properties.[3] Metal silicides are typically synthesized using high-temperature methods.[4] However, such methods do not produce nanostructures, which are needed for studying size- and dimension-dependent properties and integrating into nanoscale devices, or colloidal particles, which are useful for solution processing and for producing high-surface-area materials.[2,3,5] For these purposes, lower-temperature synthetic methods are highly desirable because they can minimize sintering and grain growth while permitting control over the growth process and therefore the size and morphology of the product.[3,5,6]

Metal silicide nanostructures have been produced using methods that include chemical vapor transport, chemical vapor deposition, ball milling, and high-temperature and -pressure reduction of metal oxide and metal salt precursors.[2,3,5,7] Solution routes have been used to grow metal silicide nanostructures off of substrates,[8] as well as to synthesize colloidal iron silicide nanoparticles.[6] However, it remains challenging to produce colloidal metal silicide nanoparticles using all-solution, ambient-pressure routes. Such solution routes, by analogy to the capabilities for other families of intermetallic compounds,[9] constitute a powerful low-temperature approach for synthesizing high-surface-area nanostructures. Such methods also offer an alternative, non-main-stream platform for the exploratory synthesis and discovery of new compounds, complementing strategies used by John Corbett to synthesize metal silicides and other intermetallic compounds throughout his distinguished career.[4,10]

Accordingly, here we report a lower-temperature solution route to colloidal metal silicide nanoparticles. Colloidal metal nanoparticles serve as reagents that transform into their corresponding metal silicides upon the injection of monophenylsilane (MPS) into trioctylamine (TOA) and squalane at 375 °C. MPS is sometimes used in the synthesis of silicon nanowires, often via higher-temperature seed-mediated vapor−liquid−solid growth processes.[11] Our prototype system for demonstrating this approach is Pd_2Si because this metal silicide is known to form readily from the interdiffusion of palladium and silicon in electronic devices[12] and because it has also been demonstrated to be catalytically active for selective hydrogenation reactions.[13] We then generalize this approach to the Cu_3Si and Ni_2Si systems. Leveraging heterogeneous catalysis as a key application that benefits from the high surface areas afforded by nanoparticles, we also show that these metal silicides function as catalysts for the hydrogen evolution reaction (HER). The HER, which involves the electrochemical reduction of aqueous protons to produce molecular hydrogen, is implicit in the function of water electrolyzers and solar fuel cells and is typically catalyzed most effectively by noble metals such as platinum.[14]

The Pd_2Si nanoparticles were synthesized by reacting palladium nanoparticles, which were produced by heating $Pd(acac)_2$ in trioctylphosphine and oleylamine at 250 °C (Figure S1 in the Supporting Information, SI),[15] with MPS in TOA and squalane at 375 °C. (Complete experimental details are included in the SI.) Briefly, the palladium nanoparticles were dispersed in TOA and then injected into a solution of squalane at 375 °C, followed by the injection of MPS dispersed in TOA. The Pd_2Si product was then washed with a mixture of chloroform and methanol and redispersed in ethanol. To remove any adventitious SiO_2, the particles were also washed with 1 M NaOH in water. Figure 1 shows a powder X-ray diffraction (XRD) pattern for the Pd_2Si particles, along with a simulated XRD pattern for Fe_2P-type Pd_2Si for comparison. The lattice parameters for the Pd_2Si product are a = 6.489 Å and c = 3.435 Å, which match well with literature values (a = 6.497 Å and c = 3.432 Å).[16] Scherrer analysis of the XRD peak widths indicates an average grain size of approximately 15 nm, which is indicative of nanocrystallinity.

A transmission electron microscopy (TEM) image of the Pd_2Si product, along with the corresponding selected-area

Special Issue: To Honor the Memory of Prof. John D. Corbett

Received: September 30, 2014
Published: November 12, 2014

ACS Publications © 2014 American Chemical Society

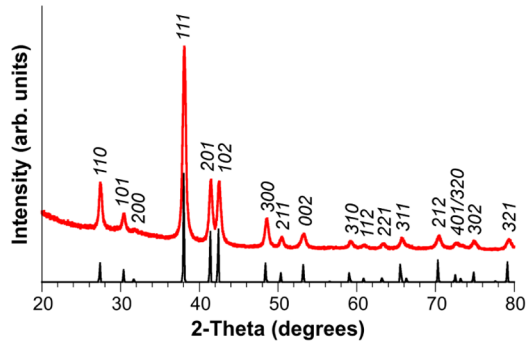

Figure 1. Powder XRD data for Pd_2Si nanoparticles: bottom (black), simulated; top (red), experimental. Indexing corresponds to Fe_2P-type Pd_2Si.

electron diffraction (SAED) pattern and energy-dispersive spectrometry (EDS) spectrum, is shown in Figure 2. The TEM

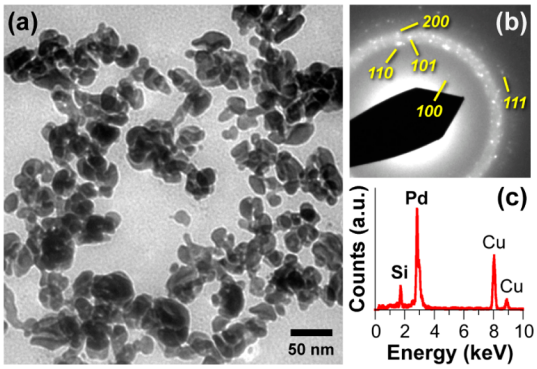

Figure 2. (a) TEM image with the corresponding (b) SAED pattern and (c) EDS spectrum for Pd_2Si nanoparticles. The copper signal in part c originates from the copper TEM grid.

image (Figure 2a) indicates that the Pd_2Si particles are nanoscopic and discrete, with a mixture of pseudospherical and multifaceted morphologies that have diameters ranging from approximately 15 to 45 nm. The average grain size of approximately 15 nm that was observed by Scherrer analysis of the XRD data is smaller than the majority of the particles observed by TEM, suggesting that the particles are polycrystalline. The SAED pattern (Figure 2b) shows diffraction spots that are consistent with the peaks expected for Fe_2P-type Pd_2Si, matching well with the bulk XRD data. The EDS data in Figure 2c indicate an approximate Pd/Si ratio of 63:37, which is consistent with the expected Pd_2Si stoichiometry.

To demonstrate the potential generality of the method, two other metal silicides were synthesized. Upon reaction of copper nanoparticles with MPS at 375 °C, Cu_3Si nanoparticles formed. Similarly, Ni_2Si nanoparticles formed from the reaction of nickel nanoparticles with MPS at 375 °C. (See Figure S1 in the SI for TEM and XRD data for the copper and nickel nanoparticles.) Figure 3 shows XRD data and TEM images for the Cu_3Si and Ni_2Si products. The XRD pattern for the Cu_3Si nanoparticles matches well with that expected for η-Cu_3Si (Figure 3a). For Ni_2Si, the XRD pattern matches well with that expected for Co_2Si-type Ni_2Si (Figure 3b). The Cu_3Si and Ni_2Si nanoparticles appear to be pseudospherical by TEM (Figures 3 and S2 in the SI), and the SAED patterns confirm their phase assignment (Figure S2 in the SI).

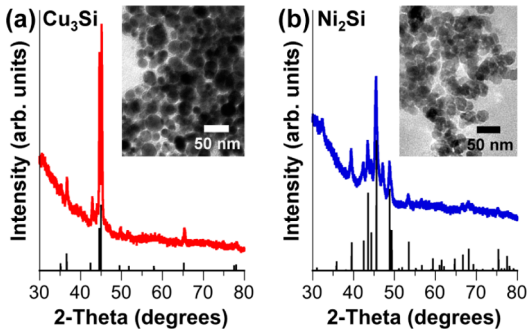

Figure 3. Powder XRD and TEM data for (a) Cu_3Si and (b) Ni_2Si nanoparticles. The bottom XRD patterns are simulated data, and the top patterns are experimental data. Minor $Cu_{0.83}Si_{0.17}$ and NiSi impurities are sometimes observed.

One advantage of solution-synthesized nanoparticles is that they have high surface areas that maximize exposure of surface sites for heterogeneous catalysis. Metal silicides catalyze several types of reactions, including hydrodesulfurization (HDS),[17] hydrogenation,[18] and hydrogen evolution.[19] In particular, Ni−Si phases are known HDS catalysts,[17] and PdSi, $NiSi_2$, and Cu_5Si phases are known HER catalysts.[19] This therefore provides an impetus to evaluate the Pd_2Si, Cu_3Si, and Ni_2Si nanoparticles as HER catalysts because a mechanistic commonality between the HDS and HER processes has been postulated based on the low energetic barrier to binding and dissociating molecular hydrogen.[14,20]

The metal silicide nanoparticles were deposited onto 0.2 cm^2 titanium foil supports (1 mg cm^{-2}) and heated in 5% H_2/Ar at 450 °C. Figure 4 shows polarization data for a bare titanium foil

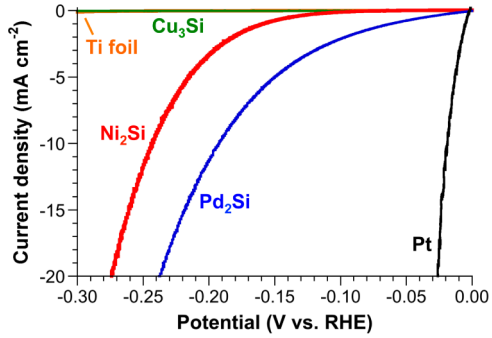

Figure 4. Polarization data (*iR*-corrected) in 0.50 M H_2SO_4 for Pd_2Si, Ni_2Si, and Cu_3Si nanoparticle films on titanium foil electrodes, as well as titanium foil and platinum mesh controls.

electrode and a platinum mesh control, as well as Pd_2Si/Ti, Cu_3Si/Ti, and Ni_2Si/Ti electrodes. The titanium foil is inactive in the potential range that was surveyed, while platinum is an excellent HER catalyst. Cu_3Si was not an active catalyst for the HER. However, Pd_2Si and Ni_2Si required overpotentials of −192 and −243 mV, respectively, to produce a current density of 10 mA cm^{-2}. The HER overpotentials for Pd_2Si and Ni_2Si revealed by this initial, preliminary evaluation are higher than those of related metal phosphide nanoparticle systems prepared and tested in a similar manner, which require −50 to −110 mV to produce a 10 mA cm^{-2} current density.[20] However, the HER overpotentials for Pd_2Si and Ni_2Si are comparable to those of other systems, including some molybdenum compounds and carbon-based nanostructures.[21] While long-term stability

dx.doi.org/10.1021/ic502394u | Inorg. Chem. 2015, 54, 707−709

remains to be established given the possible reactivity of metal silicides with aqueous acids, FeSi and $FeSi_2$ were previously found to be highly stable during sustained HER testing in H_2SO_4.[22]

In conclusion, we demonstrated the solution synthesis of several transition-metal silicides—Pd_2Si, Cu_3Si, and Ni_2Si—as colloidal nanoparticles by reacting metal nanoparticles with MPS in TOA and squalane at 375 °C. The addition of metal silicides to the list of systems that can be accessed in solution using straightforward adaptations of known colloidal nanoparticle synthetic protocols further expands this synthetic toolbox, as well as the scope of future studies that leverage their solution dispersibility and high surface areas. An initial screening indicates that Pd_2Si and Ni_2Si function as heterogeneous electrocatalysts for the HER and, as such, complement previous studies of metal silicide HER catalysts.[19]

■ ASSOCIATED CONTENT

Supporting Information

Experimental details, additional TEM and SAED data, and Tafel plots. This material is available free of charge via the Internet at http://pubs.acs.org.

■ AUTHOR INFORMATION

Corresponding Author

*E-mail: schaak@chem.psu.edu.

Notes

The authors declare no competing financial interest.

■ ACKNOWLEDGMENTS

This work was supported by the National Science Foundation Center for Chemical Innovation on Solar Fuels (Grant CHE-1305124). TEM imaging was performed in the Penn State Microscopy and Cytometry Facility (University Park, PA) at the Materials Characterization Laboratory of the Penn State Materials Research Institute.

■ DEDICATION

Dedicated to the memory of John Corbett.

■ REFERENCES

(1) Zhang, S.-L.; Ostling, M. *Crit. Rev. Solid State Mater. Sci.* **2003**, *28*, 1−129.

(2) Lin, Y.-C.; Chen, Y.; Huang, Y. *Nanoscale* **2012**, *4*, 1412−1421.

(3) Schmitt, A. L.; Higgins, J. M.; Szczech, J. R.; Jin, S. *J. Mater. Chem.* **2010**, *20*, 223−235.

(4) Kwon, Y.; Rzeznik, M. A.; Guloy, A.; Corbett, J. D. *Chem. Mater.* **1990**, *2*, 546−550.

(5) Estruga, M.; Girard, S. N.; Ding, Q.; Chen, L.; Li, X.; Jin, S. *Chem. Commun.* **2014**, *50*, 1454−1457.

(6) Dahal, N.; Chikan, V. *Chem. Mater.* **2010**, *22*, 2892−2897.

(7) (a) Lu, Q.; Hu, J.; Tang, K.; Qian, Y.; Zhou, G.; Liu, X. *Solid State Ionics* **1999**, *124*, 317−321. (b) Chen, X.; Guan, J.; Sha, G.; Gao, Z.; Williams, C. T.; Liang, C. *RSC Adv.* **2014**, *4*, 653−659.

(8) (a) Yuan, F. W.; Wang, C. Y.; Chang, S. H.; Chu, L. W.; Chen, L. J.; Tuan, H. Y. *Nanoscale* **2013**, *5*, 9875−9881. (b) Geaney, H.; Dickinson, C.; O'Dwyer, C.; Mullane, E.; Singh, A.; Ryan, K. M. *Chem. Mater.* **2012**, *24*, 4319−4325.

(9) (a) Sra, A. K.; Ewers, T. D.; Schaak, R. E. *Chem. Mater.* **2005**, *17*, 758−766. (b) Cable, R. E.; Schaak, R. E. *Chem. Mater.* **2005**, *17*, 6835−6841. (c) Chou, N. H.; Schaak, R. E. *J. Am. Chem. Soc.* **2007**, *129*, 7339−7345. (d) Bauer, J. C.; Chen, X.; Liu, Q.; Phan, T.-H.; Schaak, R. E. *J. Mater. Chem.* **2008**, *18*, 275−282.

(10) Corbett, J. D. *Inorg. Chem.* **2010**, *48*, 13−28.

(11) (a) Tuan, H.; Lee, D. C.; Hanrath, T.; Korgel, B. A. *Nano Lett.* **2005**, *5*, 681−684. (b) Heitsch, A. T.; Hessel, C. M.; Akhavan, V. A.; Korgel, B. A. *Nano Lett.* **2009**, *9*, 3042−3047.

(12) (a) Bower, R. W.; Sigurd, D.; Scott, R. E. *Solid-State Electron.* **1973**, *16*, 1461−1471. (b) Joshi, R. K.; Yoshimura, M.; Tanaka, K.; Ueda, K.; Kumar, A.; Ramgir, N. *J. Phys. Chem. C* **2008**, *112*, 13901−13904.

(13) Zaheer, M.; Motz, G.; Kempe, R. *J. Mater. Chem.* **2011**, *21*, 18825−18831.

(14) Morales-Guio, C. G.; Stern, L.-A.; Hu, X. *Chem. Soc. Rev.* **2014**, *43*, 6555−6569.

(15) Kim, S.; Park, J.; Jang, Y.; Chung, Y.; Hwang, S.; Hyeon, T.; Kim, Y. W. *Nano Lett.* **2003**, *3*, 1289−1291.

(16) Aronsson, B.; Nylund, A. *Acta Chem. Scand.* **1960**, *14*, 1011.

(17) Chen, X.; Liu, X.; Wang, L.; Li, M.; Williams, C. T.; Liang, C. *RSC Adv.* **2013**, *3*, 1728−1731.

(18) (a) Panpranot, J.; Phandinthong, K.; Sirikajorn, T.; Arai, M.; Praserthdam, P. *J. Mol. Catal. A: Chem.* **2007**, *261*, 29−35. (b) Chen, X.; Li, M.; Guan, J.; Wang, X.; Williams, C. T.; Liang, C. *Ind. Eng. Chem. Res.* **2012**, *51*, 3604−3611.

(19) (a) Vijh, A. K.; Belanger, G.; Jacques, R. *Int. J. Hydrogen Energy* **1990**, *15*, 789−794. (b) Vijh, A. K.; Belanger, G. *J. Mater. Sci. Lett.* **1995**, *14*, 982−984. (c) Faber, M. S.; Jin, S. *Energy Environ. Sci.* **2014**, *7*, 3519−3542.

(20) (a) Popczun, E. J.; Read, C. G.; Roske, C. W.; Lewis, N. S.; Schaak, R. E. *J. Am. Chem. Soc.* **2014**, *53*, 5427−5430. (b) Popczun, E. J.; Read, C. G.; Roske, C. W.; Lewis, N. S.; Schaak, R. E. *Angew. Chem., Int. Ed.* **2014**, *53*, 5427−5430. (c) McEnaney, J. M.; Crompton, J. C.; Callejas, J. F.; Popczun, E. J.; Biacchi, A. J.; Lewis, N. S.; Schaak, R. E. *Chem. Mater.* **2014**, *26*, 4826−4831. (d) McEnaney, J. M.; Crompton, J. C.; Callejas, J. F.; Popczun, E. J.; Read, C. G.; Lewis, N. S.; Schaak, R. E. *Chem. Commun.* **2014**, *50*, 11026−11028. (e) Callejas, J. C.; McEnaney, J. M.; Read, C. G.; Crompton, J. C.; Biacchi, A. J.; Popczun, E. J.; Gordon, T. R.; Lewis, N. S.; Schaak, R. E. *ACS Nano* **2014**, DOI: DOI: 10.1021/nn5048553.

(21) (a) Zou, X.; Huang, X.; Goswami, A.; Silva, R.; Sathe, B. R.; Mikmeková, E.; Asefa, T. *Angew. Chem., Int. Ed.* **2014**, *53*, 4372−4376. (b) Vrubel, H.; Hu, X. *Angew. Chem., Int. Ed.* **2012**, *51*, 12703−12706.

(22) Vijh, A. K.; Belanger, G.; Jacques, R. *Mater. Chem. Phys.* **1988**, *20*, 529−538.